Molecular structure and chirality detection by fourier transform microwave spectroscopy

Molecular Structure and Chirality Detection by Fourier Transform Microwave Spectroscopy

Simon Lobsiger,[†] Cristobal Perez,[†] Luca Evangelisti,[†,‡] Kevin K. Lehmann,*[,†] and Brooks H. Pate*[,†]

[†]Department of Chemistry, University of Virginia, McCormick Road, Charlottesville, Virginia 22904, United States

[‡]Department of Chemistry "G. Ciamician", University of Bologna, Via Selmi 2, Bologna, 40126, Italy

Supporting Information

ABSTRACT: We describe a three-wave mixing experiment using time-separated microwave pulses to detect the enantiomer-specific emission signal of the chiral molecule using Fourier transform microwave (FTMW) spectroscopy. A chirped-pulse FTMW spectrometer operating in the 2−8 GHz frequency range is used to determine the heavy-atom substitution structure of solketal (2,2-dimethyl-1,3-dioxolan-4-yl-methanol) through analysis of the singly substituted ^{13}C and ^{18}O isotopologue rotational spectra in natural abundance. A second set of microwave horn antennas is added to the instrument design to permit three-wave mixing experiments where an enantiomer-specific phase of the signal is observed. Using samples of *R*-, *S*-, and racemic solketal, the properties of the three-wave mixing experiment are presented, including the measurement of the corresponding nutation curves to demonstrate the optimal pulse sequence.

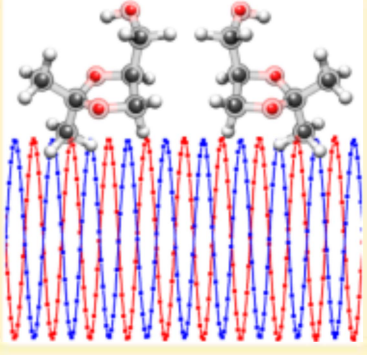

Chirality has played a central role in chemistry, biochemistry, and biology since it was discovered by Pasteur in 1848.[1] The vast majority of biological processes, such as molecular recognition,[2] enzymatic catalysis, and metabolic reactions are enantioselective. Thus, the development of measurement techniques to distinguish enantiomers is an important area of analytical chemistry. Spectroscopy techniques that can directly characterize chirality include optical rotation (OR), circular dichroism (CD), vibrational circular dichroism (VCD), and Raman optical activity (ROA).[3] These chiroptical methods probe the interference between the electric dipole transition moment and the usually weak magnetic dipole transition moment and are, therefore, not very sensitive.

A different approach using Fourier transform rotational spectroscopy has recently been reported by Patterson, Schnell, and Doyle[4] and has been discussed theoretically by Hirota, who described the behavior of the rotational wave functions in triple resonance measurements.[5] The measurement uses the fact that enantiomers can be distinguished by the sign of the products of the molecular dipole moment projections on the principal axis system of molecular rotation. Three-wave mixing can be used to generate a coherent molecular rotational signal that can be detected in Fourier transform microwave (FTMW) spectroscopy, and enantiomers can be distinguished by the phase of this signal. Because both enantiomers have coherent emission at the same frequency, a net signal is only detected when there is an enantiomeric excess.

In the landmark paper of Patterson, Schnell, and Doyle,[4] the chiral signal was generated by polarizing the molecules using microwave radiation that is resonant with an electric dipole transition while a nonresonant DC electric field, perpendicularly oriented to the polarization of the first microwave field, is applied. Once the DC field is switched off, the combination of these two fields generates a free induction decay (FID) that is perpendicularly polarized to both the DC and the microwave fields.

More recently, Shubert et al.,[6] Grabow,[7] and Patterson and Doyle[8] have discussed the excitation more generally and shown that the three-wave mixing experiment can be performed with two, resonant pulses instead of the DC field used in the first report. Details of this approach as applied in the current work can be found in the Supporting Information. This work follows previous descriptions of three-wave mixing or higher-wave interactions (sum frequency generation, SFG) that have been proposed as methods to selectively excite, purify, or even interconvert enantiomers.[9−11] A major advantage of the double resonance technique is that the generated FID is at a frequency with no background. Another is that it is much easier to rapidly switch off the microwave pulses than short the high-voltage Stark electrodes, and the microwave pulses can be reapplied faster than the Stark electrodes can be recharged. Moreover, there is no dephasing in either excitation or emission due to the presence of multiple Stark-shifted transitions, thereby reducing signal. However, there is a reduction of the signal due to imperfect phase matching, which can be viewed as a spatial dephasing.[12] The FTMW three-wave mixing method has been successfully applied to chiral samples with one[6,13] and even expanded to systems with two[14] stereogenic centers in experiments where one excitation pulse is at radio frequenices.

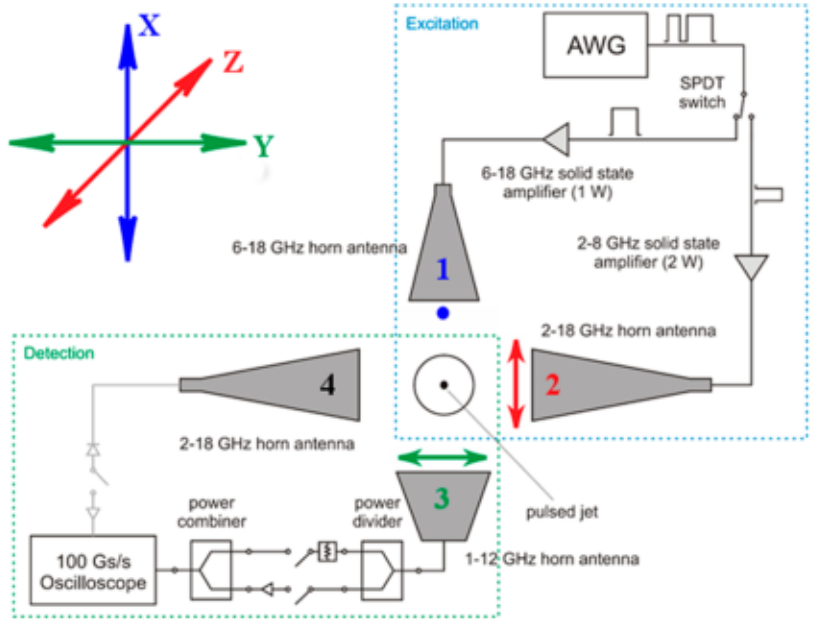

Figure 1. Schematic of the 2−8 GHz CP-FTMW spectrometer with chirality detection capabilities. This schematic is divided into two parts, excitation and detection. The orientation of the polarized microwave fields used in the three-wave mixing experiment is highlighted in the top-left inset. See the text for more details.

Here, we show how a chirped-pulse Fourier transform microwave (CP-FTMW) spectrometer[15] can easily be adapted for chiral-sensitive measurements via three-wave mixing with the inclusion of an extra set of microwave horns. In this design, both of the resonant, single-frequency excitation pulses in the three-wave mixing experiment are at microwave frequencies. The use of microwave instead of radio frequency pulses makes it easier to control the excitation pulses in the measurement. We also use time-separated excitation pulses, instead of having them overlap in time, and this allows us to demonstrate the optimal pulse sequence for chiral FTMW spectroscopy.[7]

The design of our spectrometer is shown in Figure 1, and the details of the basic CP-FTMW spectrometer have been presented elsewhere.[15] We focus on the new components that enable enantiomer-specific detection. As shown in Figure 1, the two excitation pulses are generated using an arbitrary waveform generator (Tektronix AWG 7122B with channel interleave), which enables high phase stability and repeatability. The two microwave pulses are separated using a single pole double throw (SPDT) switch (Sierra Microwave Technology SFD0526) and are amplified by two solid-state amplifiers (Microwave Power L0618 and L0208) with frequency coverage of 6−18 GHz and 2−8 GHz, respectively. Once amplified, each pulse is broadcast into the vacuum chamber by a microwave horn antenna; these broadcast horns are labeled 1 and 2 in Figure 1. One pulse is broadcast by one of the horns of our conventional broad-band spectrometer (Q-Par Angus WBH 2-18-NHG: horn antenna 1), while the other is by a waveguide horn (ATM-650-442-C1; horn antenna 2). The essential feature for chiral FTMW spectroscopy is that the three microwave signals (the two excitation pulses and the emitted coherent FID signal) have mutually orthogonal polarization. The selections of excitation pulse and FID detection polarizations are denoted in Figure 1 and color coded using the axis system shown in the top left. Following excitation of the sample, the coherent FID is collected by a third horn (ATM 1-12-440EM-NF; horn antenna 3), amplified, and then digitized at 50 Gs/s using a high-speed oscilloscope (Tektronix DPO 73304D). In order to collect the two excitation pulses and the molecular signal on a single digitizer channel, a combination of power divider/power combiner is placed at the detection end of the spectrometer, allowing attenuation of the microwave pulses to levels that the digitizer can safely handle and amplification of the FID.

Solketal (2,2-dimethyl-1,3-dioxolan-4-yl-methanol), the molecule chosen for this study, is a protected glycerol that is used in the synthesis of triglycerides. (R) and (S) enantiomers (>97% ee) as well as the racemic mixture were purchased from Sigma-Aldrich and used without further purification.

We first measured the broad-band spectrum in the 2−8 GHz frequency region, shown in Figure 2, using the CP-FTMW instrument. A complete set of a-, b- and c-type rotational transitions were fit to the Watson asymmetric top rotational Hamiltonian using SPFIT/SPCAT.[16] The experimental rotational constants as well as a complete list of frequencies can be found in the Supporting Information. The signal-to-noise ratio was high enough to observe the spectra of all singly substituted heavy atom (^{13}C, ^{18}O) species in natural abundance (see the Supporting Information) from which we obtained the full heavy-atom substitution (r_s) structure of the molecule through the Kraitchman equations.[17] In Figure 2, the resulting experimental atom positions are compared to those obtained from quantum chemistry calculations at the M06-2X/6-311++G(d,p) level of theory. These calculations also yielded the dipole moment components in the principal axis system of the molecule, $|\mu_a| = 1.8$ D, $|\mu_b| = 1.2$ D, and $|\mu_c| = 0.2$ D.

One of the possible rotational transition cycles for solketal is shown in Figure 2. A brief description of the creation of an enantiomer-specific chiral signal is presented here. Detailed expressions for the chiral signature in the three-wave mixing experiment can be found in the Supporting Information. We first apply a resonant, single-frequency microwave pulse with X polarization (c-type transition). This pulse transforms the

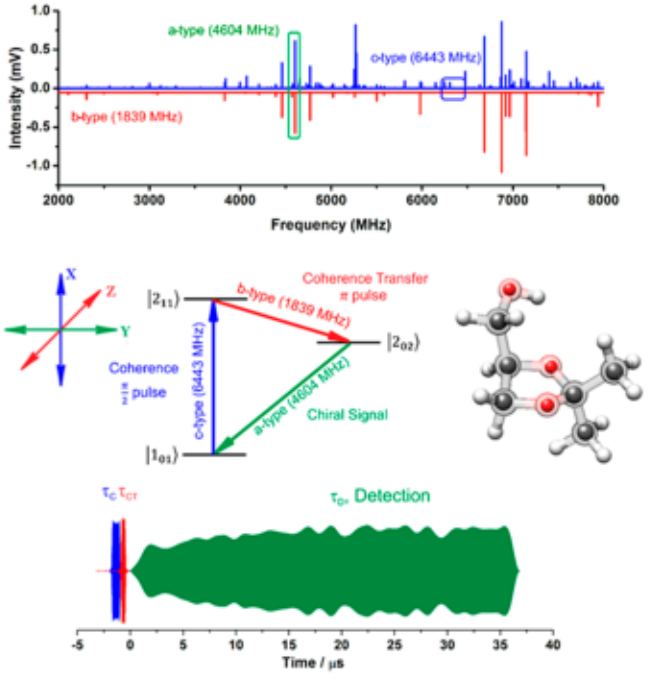

Figure 2. The top panel shows the experimental CP-FTMW spectrum of solketal in the 2−8 GHz frequency region. The blue trace is the experimental spectrum, while the red one is a 1.5 K (rotational temperature) simulation. The spectrum is the Fourier transform of 400000 FIDs, co-added in the time domain. The three-wave mixing scheme is shown in the middle. The broad-band signal measured by the high-speed digitizer is diplayed at the bottom. It shows the two excitation pulses (blue and red) and the enantiomer-dependent molecular FID (green) corresponding to (*S*)-solketal. The excitation pulses and molecular FID are digitized using different gain levels to place them on the same scale. The modulations of the FID envelope are caused by "beating" with other signals in the full bandwidth of the digitizer, and these mainly come from spurious signals within the digital oscilloscope. A comparison of experimental atom positions with the theoretical structure obtained from calculations at the M06-2X/6-311++G(d,p) level is shown on the middle-right. In this image, the smaller solid spheres represent the experimental atom positions obtained from analysis of the rotational spectra of the solketal isotopologues.

population difference into coherence, creating a superposition state with the form

$$|\Psi\rangle = \cos\left(\frac{\Theta_{\text{Rabi}}}{2}\right) e^{-iE(1_{01})t/\hbar}|1_{01}\rangle + i\sin\left(\frac{\Theta_{\text{Rabi}}}{2}\right) e^{-iE(2_{11})t/\hbar}|2_{11}\rangle \quad (1)$$

with the Rabi flip angle defined as

$$\Theta_{\text{Rabi}} = \omega_{\text{Rabi}} t_{\text{pulse}} = \frac{\langle\mu\rangle E}{\hbar} t_{\text{pulse}} \quad (2)$$

where E is the electric field strength of the resonant microwave pulse, $\langle\mu\rangle$ is the transition dipole matrix element between the initial and intermediate states, and t_{pulse} is the length of the excitation pulse. In this way, the superposition state coefficients contain the signed dipole moment information. The optimal coherence is created for a Rabi flip angle of $\pi/2$. Note that for rotational spectroscopy, the transition moments for the different projections of the angular momentum on the space-fixed x-axis depend on the projection quantum number, M_J.[18]

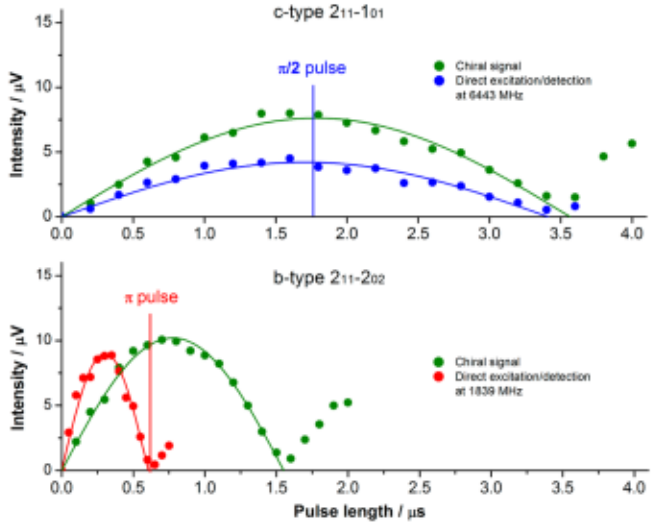

Figure 3. Molecular rotational signals for the chiral signal and the coherence and coherence transfer pulses are shown as the pulse duration is varied. In the top panel, where optimization of the coherence transfer pulse is shown, the duration of the resonant c-type pulse at 6443 MHz is fixed at the optimal $\pi/2$ pulse duration. In the bottom panel, the resonant excitation for the b-type coherence transfer pulse at 1839 MHz is kept constant at the approximate π pulse condition.

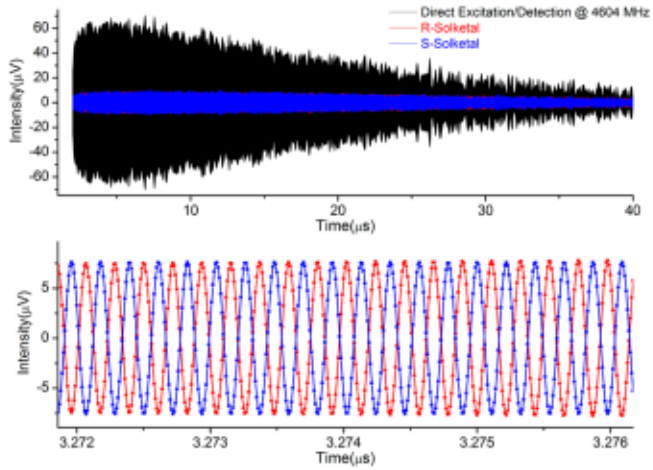

Figure 4. Filtered molecular FIDs obtained at 4604 MHz are shown. The black trace is the signal when the transition is directly excited/detected. Red and blue traces are the chiral signals using the three-wave mixing experiment. The bottom panel shows a small interval of the total FID, highlighting the phase displacement between enantiomers. The actual digitizer data points (50 Gs/s) are shown by the small circles on each signal in this expanded time scale plot. The filtering of the signal measured with the high-speed digitizer removes the beating effects in the FID envelope that are caused by spurious signals, as mentioned in the caption for Figure 2

Therefore, an exact "$\pi/2$ pulse" cannot be achieved for all rotational levels, and the $\pi/2$ pulse terminology denotes the pulse duration for maximum coherence. The second resonant field with Z polarization (b-type transition), in additional to creating a coherence between states $|2_{11}\rangle$ and $|2_{02}\rangle$, transfers some of the existing coherence between states $|1_{01}\rangle$ and $|2_{11}\rangle$ into a coherence between states $|1_{01}\rangle$ and $|2_{02}\rangle$. This coherence is optimized when the Rabi flip angle for the second step of excitation is equal to π, with a duration τ_{CT} in this case. Again,

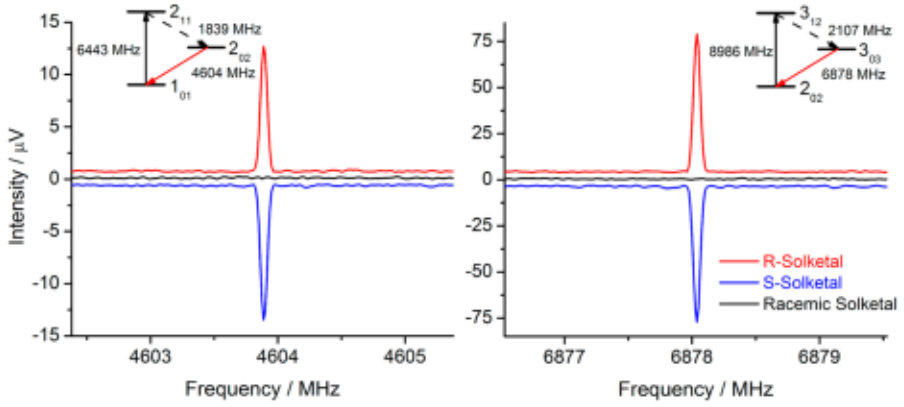

Figure 5. Enantiomer-dependent chiral signals for two different cycles containing the transitions (A) $|1_{01}\rangle \rightarrow |2_{11}\rangle$ = 6443 MHz, $|2_{11}\rangle \rightarrow |2_{02}\rangle$ = 1839 MHz, and $|2_{02}\rangle \rightarrow |1_{01}\rangle$ = 4604 MHz and (B) $|2_{02}\rangle \rightarrow |3_{12}\rangle$ = 8986 MHz, $|3_{12}\rangle \rightarrow |3_{03}\rangle$ = 2107 MHz, and $|3_{03}\rangle \rightarrow |2_{02}\rangle$ = 6878 MHz. The spectra are the Fourier transforms of (A) 100000 and (B) 50000 FIDs. Both red and blue traces include a small offset to facilitate visualization.

the M_J dependence of the transition moments prevents exact π pulse excitation for all levels.

Following the coherence transfer pulse, the wave function that describes the system has the form

$$|\Psi\rangle = c_1(t)|1_{01}\rangle + c_2(t)|2_{11}\rangle + c_3(t)|2_{02}\rangle \quad (3)$$

and it will now generate coherent emission at the frequency of the $2_{02}-1_{01}$ rotational transition. The molecular signal appears Y-polarized (a-type) under the assumed laboratory frame axes and is collected for 40 μs, τ_D.

The design of the optimal pulse sequence takes into account the following points. First, the chiral signal is proportional to the population difference between the pair of states first pumped. Thus, it is maximized if the transition with the largest population difference (i.e., highest frequency) is pumped first. Because there is usually sufficient microwave power, it is convenient to choose an R-branch ($\Delta J = +1$) transition with selection rules of the smallest dipole moment projection for this pulse (c-type for Solketal). Second, the chiral signal is also proportional to the transitions dipole moment component. Therefore, it is desirable to monitor the rotational transition with the highest dipole moment, a-type in the present study, and at high molecular frequency ($\Delta J = -1$). Additionally, the cycle must contain a Q-branch transition, in our case a b-type.

Optimization of the chiral signal is illustrated in Figure 3 where the molecular rotational signals are monitored as a function of pulse duration to determine the optimal Rabi flip angles of the coherence ($\pi/2$) and the coherence transfer (π) pulses. Two separate experiments were performed for each excitation pulse. First, the c-type transition was directly excited and detected by increasing the pulse length in 200 ns intervals from 200 to 3500 ns, as shown in the blue trace of the bottom panel of Figure 3. The signal reaches a maximum value for an excitation pulse of 1.75 μs (τ_C), which corresponds to a $\pi/2$ pulse. Second, we used the same set of pulses but monitored the chiral signal. The duration of the second excitation pulse was kept fixed at 500 ns. As can be seen in Figure 3 (green trace), the chiral signal was maximized when a $\pi/2$ pulse was applied. Analogously, we determined the optimal pulse length of the coherence transfer pulse (b-type transition) by using 50 ns increments and directly detecting at 1839 MHz. The length for a $\pi/2$ pulse was reached at approximately 375 ns. However, when monitoring the chiral signal, the optimal pulse duration was at 750 ns, that is, a π pulse, highlighted in red in Figure 3.

The chiral signal for the three-wave mixing experiment that uses optimal, time-separated excitation pulses is compared to the signal of the transition excited in a single-color experiment (4604 MHz and pulse length of 150 ns) in Figure 4. The signal variation of the a-type transition as a function of pulse duration is available in the Supporting Information. A small portion of the digitized signal for both enantiomers (waves shifted by π radians) is presented in the bottom panel of Figure 4. This signal was isolated from the broad-band signal using a digital band-pass filter. Figure 5 shows the Fourier transform of the chiral signals for both enantiomers as well as the racemic mixture (black), which does not radiate at the difference frequency. The spectrum of (*S*)-solketal is plotted to the negative for a better comparison of the signal levels. The signal-to-noise ratios of the two cycles shown in Figure 5 are 50:1 (A) and 110:1 (B).

The performance of a microwave spectrometer capable of high-sensitivity pure rotational spectroscopy, for spectral analysis and structure determination using natural abundance isotopic substitution, and for three-wave mixing experiments for chiral analysis has been described. Unlike previous implementations of chiral FTMW spectroscopy, this instrument uses high-frequency microwave pulses and applies these pulses in an optimal, time-separated "$\pi/2-\pi$" sequence. The resulting chiral signals in the three-wave mixing experiments have comparable signal levels to single-color rotational spectroscopy experiments giving a high-sensitivity chiral signature. The phase behavior of the chiral signal for different enantiomers and the related zero signal strength for a racemic mixture caused by destructive interference have been demonstrated. In principle, absolute configurations of chiral molecules can be determined from the chiral signal phase and quantum chemistry calculation of the dipole moment. However, we were unable to achieve absolute phase determination in the current experiments. We do observe that the signals are phase-reproducible in different measurements over different days. This result suggests that more careful calibration of phase shifts induced by microwave circuit components and the geometry of the horn antenna receiver relative to the sample interaction region will produce a method for the reliable determination of absolute configuration.

The generation of a chiral signal in the sample also requires phase-matching conditions to be met, and it might be expected that the chiral signal will diminish as higher frequencies are used in the measurement (where wavelengths become short compared to the sample size).[12] The strongest chiral signals

have been observed for the highest transition frequencies in this work. The physical dimensions of the pulsed jet expansion may reduce the phase-matching requirements, as discussed in the Supporting Information. Evidence of some form of volume restriction for the chiral signal is found in the longer dephasing time of the chiral signal relative to the single-color measurement that can be discerned in Figure 4. Phase calibration and modeling of signals generated by spatially restricted samples, like those produced in a pulsed jet expansion, are directions for future work.

■ ASSOCIATED CONTENT

Supporting Information

Explicit expression for three-level mixing, rotational constants of normal species, ^{13}C and ^{18}O isotopologues, Cartesian coordinates of ab initio calculations, results from Kraitchman analysis, and line lists of assigned transitions. This material is available free of charge via the Internet at http://pubs.acs.org.

■ AUTHOR INFORMATION

Corresponding Authors

*E-mail: lehmann@virginia.edu (K.K.L).
*E-mail: brookspate@virginia.edu (B.H.P.).

Notes

The authors declare the following competing financial interest(s): Brooks H. Pate is Chief Technical Officer for BrightSpec and has restricted stock in the company. BrightSpec has an exclusive license with Harvard University for chiral analysis using three-wave mixing FTMW spectroscopy.

■ ACKNOWLEDGMENTS

This work was supported by U.S. National Science Foundation (NSF) Grants CHE-0960074 and CHE-1213200. S.L. acknowledges support from the Swiss National Science Foundation (PBBEP2-144907). L.E. was supported by Marie Curie fellowship PIOF-GA-2012-328405.

■ REFERENCES

(1) Gal, J. Louis Pasteur, Language, and Molecular Chirality. I. Background and Dissymmetry. *Chirality* **2011**, *23*, 1−16.
(2) Baron, R.; McCammon, J. A. Molecular Recognition and Ligand Association. *Annu. Rev. Phys. Chem.* **2013**, *64*, 151−175.
(3) Nafie, L. A. Infrared and Raman Vibrational Optical Activity: Theoretical and Experimental Aspects. *Annu. Rev. Phys. Chem.* **1997**, *48*, 357−386.
(4) Patterson, D.; Schnell, M.; Doyle, J. M. Enantiomer-Specific Detection of Chiral Molecules via Microwave Spectroscopy. *Nature* **2013**, *497*, 475−477.
(5) Hirota, E. Triple Resonance for a Three-Level System of a Chiral Molecule. *Proc. Jpn. Acad., Ser. B* **2012**, *88*, 120−128.
(6) Shubert, V. A.; Schmitz, D.; Patterson, D.; Doyle, J. M.; Schnell, M. Identifying Enantiomers in Mixtures of Chiral Molecules with Broadband Microwave Spectroscopy. *Angew. Chem., Int. Ed.* **2014**, *53*, 1152−1155.
(7) Grabow, J.-U. Fourier Transform Microwave Spectroscopy: Handedness Caught by Rotational Coherence. *Angew. Chem., Int. Ed.* **2013**, *52*, 11698−11700.
(8) Patterson, D.; Doyle, J. M. Sensitive Chiral Analysis via Microwave Three-Wave Mixing. *Phys. Rev. Lett.* **2013**, *111*, 023008.
(9) Belkin, M. A.; Kulakov, T. A.; Ernst, K.-H.; Yan, L.; Shen, Y. R. Sum-Frequency Vibrational Spectroscopy on Chiral Liquids: A Novel Technique to Probe Molecular Chirality. *Phys. Rev. Lett.* **2000**, *85*, 4474−4477.
(10) Fischer, P.; Wiersma, D. S.; Righini, R.; Champagne, B.; Buckingham, A. D. Three-Wave Mixing in Chiral Liquids. *Phys. Rev. Lett.* **2000**, *85*, 4253−4256.
(11) Král, P.; Shapiro, M. Cyclic Population Transfer in Quantum Systems with Broken Symmetry. *Phys. Rev. Lett.* **2001**, *87*, 183002.
(12) Fischer, P.; Wiersma, D. S.; Righini, R.; Champagne, B.; Buckingham, A. D. Three-Wave Mixing in Chiral Liquids. *Phys. Rev. Lett.* **2000**, *85*, 4253−4256.
(13) Patterson, D.; Schnell, M. New Studies on Molecular Chirality in the Gas Phase: Enantiomer Differentiation and Determination of Enantiomeric Excess. *Phys. Chem. Chem. Phys.* **2014**, *16*, 11114−11123.
(14) Alvin Shubert, V.; Schmitz, D.; Schnell, M. Enantiomer-Sensitive Spectroscopy and Mixture Analysis of Chiral Molecules Containing Two Stereogenic Centers — Microwave Three-Wave Mixing of Menthone. *J. Mol. Spectrosc.* **2014**, *300*, 31−36.
(15) Pérez, C.; Lobsiger, S.; Seifert, N. A.; Zaleski, D. P.; Temelso, B.; Shields, G. C.; Kisiel, Z.; Pate, B. H. Broadband Fourier Transform Rotational Spectroscopy for Structure Determination: The Water Heptamer. *Chem. Phys. Lett.* **2013**, *571*, 1−15.
(16) Pickett, H. M. The Fitting and Prediction of Vibration−Rotation Spectra with Spin Interactions. *J. Mol. Spectrosc.* **1991**, *148*, 371−377.
(17) Kraitchman, J. Determination of Molecular Structure from Microwave Spectroscopic Data. *Am. J. Phys.* **1953**, *21*, 17−24.
(18) Gordy, W.; Cook, R. L.; *Microwave Molecular Spectra*, 3rd ed.; Wiley: New York, 1984.